第 48 卷 第 2 期/2021 年 1 月/中国激光 研究论文

中国激光

超疏水聚偏氟乙烯的激光加工

李纪超[1]，陈招弟[1]，韩冬冬[1*]，张永来[1]，孙洪波[2]

[1]吉林大学电子科学与工程学院集成光电子学国家重点实验室，吉林 长春 130012；

[2]清华大学精密仪器系精密测试技术及仪器国家重点实验室，北京 100084

摘要 以激光加工工艺为基础，仿照荷叶超疏水表面对聚偏氟乙烯薄膜进行加工，实现了具有微结构、低表面能的超疏水聚偏氟乙烯表面，该方法简便且不涉及化学试剂。实验结果表明，激光处理后的聚偏氟乙烯薄膜表面具有类似荷叶表面的微乳突结构，碳元素与氟元素的含量(原子数分数)比由 1.2 提高至 11.5。聚偏氟乙烯薄膜的水滴接触角约为 82°，激光处理过的聚偏氟乙烯薄膜的水滴接触角约为 150°，这表明经激光处理后的聚偏氟乙烯材料具有超疏水特点。

关键词 激光技术；聚偏氟乙烯；超疏水；仿生表面；微纳结构

中图分类号 V261.8 **文献标志码** A **doi**：10.3788/CJL202148.0202002

1 引 言

自然界中存在着各种各样的奇妙现象，如水滴在荷叶表面自由滚动、水滴在水稻叶表面各向异性滚动、水滴在猪笼草口缘区单向运动现象[1-2]。随着科学技术的发展，近年来对特异浸润性表面的研究也受到了人们的关注，并在日常生活、工业生产等领域产生了巨大的经济价值。如超疏水表面具有自清洁性、抗结冰性等特点，已被广泛应用于生物、工业、微机械等领域[3]。

固体表面的超疏水性质通常与表面微纳结构和化学组分有关[4-7]。一方面，表面微纳结构可以减小水滴与固体表面的接触面积，提高疏水性能，常用模板法、光刻、电镀、自组装、化学腐蚀等工艺在固体表面引入微纳结构。另一方面，通过化学试剂改变材料表面的化学组分，可降低材料表面能，提高疏水性能。从制备方法角度来看，激光加工技术具有易于控制、精度高等优点[8-10]，被广泛应用于多种结构和器件的制备[11-17]。且激光加工技术具有良好的适用性[18-21]，不论是硬质材料还是柔性材料，都可以通过调控激光加工参数制备特定微纳结构和表面改性[22-25]。

有机材料的表面能较低，因此超疏水有机材料的制备成为超疏水领域研究的热点。如 Yuan 等[26]以芋头叶为模板，制备出具有与天然芋头叶乳突类似的聚苯乙烯膜，表面的水滴接触角为 158°±1.6°；Oktay 等[27]通过静电纺丝技术制备出基于聚酰亚胺硅氧烷复合材料的电纺薄膜，薄膜表面显示出与荷叶相似的超疏水性，可作为自清洁薄膜；Gong 等[28]创新性地将聚二甲硅氧烷(PDMS)倒入激光烧蚀出的不锈钢板中固化，得到静态接触角可达 155°的超疏水 PDMS 薄膜；Wang 等[29]用激光直接处理 PDMS 表面，使 PDMS 发生碳化，碳化后的表面具有超疏水性。

聚偏氟乙烯(PVDF)是一种常见的有机高分子共聚物，具有良好的柔性、耐腐蚀性、压电性等优点[30]。迄今为止，共混改性、表面处理改性等方式已被用于制备基于 PVDF 的超疏水表面，但通常需要特殊的化学试剂或复杂的工艺设备[31-34]。针对上述问题，本文提出以激光加工技术为基础，仿荷叶的超疏水表面对 PVDF 薄膜进行加工，实现了具有微结构、低表面能的超疏水聚偏氟乙烯，处理过程简便且不涉及化学试剂。

收稿日期：2020-09-09；**修回日期**：2020-10-11；**录用日期**：2020-11-12

基金项目：国家重点研发计划(2017YFB1104300)、国家自然科学基金(61905087，61935008，61775078，61590930)、吉林省科技发展规划(20180101061JC)、国防科创新特区项目、中国博士后科学基金(2020T130237，2020M670850)、中央高校基本科研业务费专项资金(2020-JCXK-18)

* **E-mail**：handongdong@jlu.edu.cn

2 实验部分

2.1 实验材料及设备

PVDF 粉末材料购买于 Sigma-Aldrich 公司，N,N—二甲基甲酰胺(DMF)购买于上海阿拉丁生化科技股份有限公司，用于 PVDF 粉末的溶解及成膜。激光器为半导体连续激光器，波长为 450 nm，焦距为 50 mm，光斑直径约为 70 μm，采用单向线扫描方式，扫描速度为 3 mm/s，最大输出功率为 3000 mW。研究不同激光功率处理 PVDF 表面对疏水性能的影响时，采用不用激光功率(300，600，900，1200，1500，1800，2100，2400，2700 mW)对薄膜表面进行激光处理，得到激光处理过的 PVDF 薄膜材料(L-PVDF)。激光处理的面积为 10 mm×10 mm，加工时间约为 3 min，用于静态接触角(CA)测试。用静态接触角测试仪(SDC-350，SIN DIN Corporation)测量薄膜材料表面的水滴静态接触角，液体体积为 6 μL。采用激光共聚焦显微镜(CLSM，OLS4100)、冷场发射扫描电子显微镜(SEM，JSM-7500)对表面结构进行观察，用 X 射线光电子能谱(XPS，ESCALAB 250 spectrometer)测试样品表面元素的变化情况。

2.2 PVDF 薄膜以及超疏水 PVDF 薄膜的制备

将 PVDF 粉末与 DMF 溶剂按照 1 g∶8 mL 的比例进行混合，搅拌至粉末溶于液体后，放置于超声清洗机中进行超声处理(1 h)，使 PVDF 粉末分散更均匀，同时去除混合过程中引入的气泡，得到流动性、成膜性较好的均匀混合物。

将混合物滴在玻璃基底上，混合物在温度为 80 ℃时热烘干处理 10～15 min 后成膜。通过 SEM 观察，制备的 PVDF 薄膜厚度约为 17 μm。将 PVDF 薄膜放置于半导体连续激光器的加工区域，在合适的功率下对薄膜表面进行激光处理，得到 L-PVDF 材料，加工区域的大小根据需求面积设置。同时对未加工的 PVDF 薄膜也进行裁剪，得到相同面积(10 mm×10 mm)的 PVDF 薄膜材料，用于实验测试、对比分析。

3 分析与讨论

3.1 荷叶表面形貌观察

如图 1(a)所示，水滴可以在荷叶表面自由滚动。利用静态接触角测试仪测试荷叶表面水滴的接触角，发现荷叶的水滴静态接触角可达 150°，具有超疏水特点，如图 1(b)所示。为进一步探究荷叶表面的超疏水特点，分别采用 CLSM 和 SEM 对荷叶表面进行观察分析。图 1(c)为荷叶表面的 CLSM 图像，可以发现，荷叶表面存在许多直径不超过 10 μm、高为 5～10 μm 的乳突。图 1(d)、图 1(e)为荷叶表面的 SEM 图像，可以发现，荷叶表面具有直径约为 3～5 μm 的乳突。乳突的存在可以有效减少水滴与荷叶表面的接触面积，达到超疏水效果[35-36]。

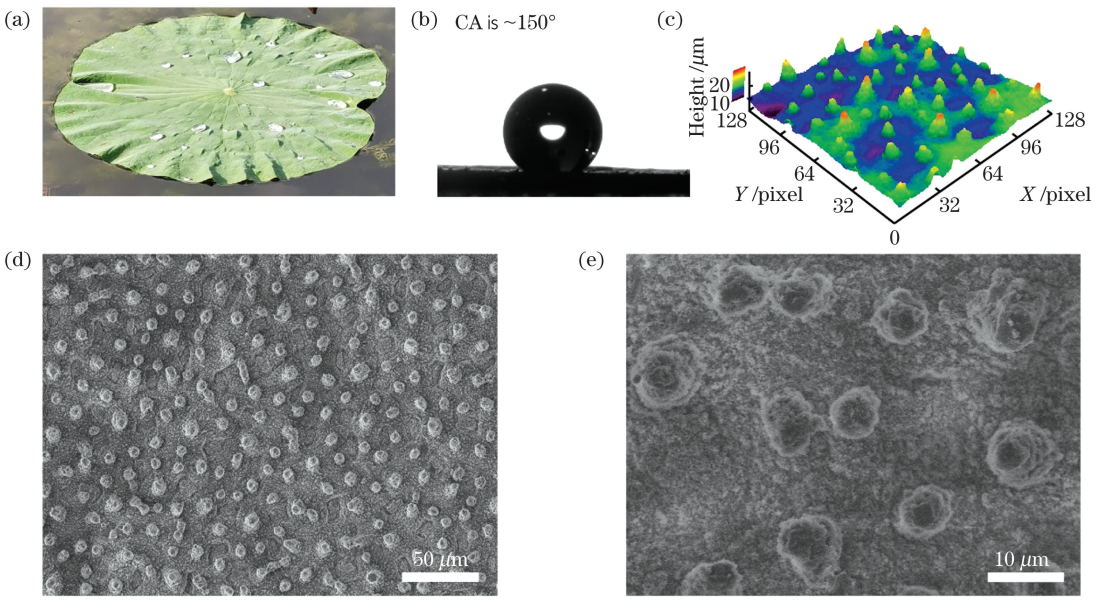

图 1 荷叶疏水性能的测试。(a)实物图；(b)静态接触角；(c) CLSM 图像；(d) SEM 图像(50 μm)；(e) SEM 图像(10 μm)

Fig. 1 Test of the hydrophobicity of lotus leaf. (a) Photograph; (b) static contact angle; (c) CLSM image; (d) SEM image (50 μm); (e) SEM image (10 μm)

3.2　PVDF 与 L-PVDF 表面形貌对比

图 2(a)、图 2(b)分别为激光加工系统和激光处理 PVDF 材料表面的加工流程示意图。首先，将 PVDF 液体滴在玻璃基底表面，烘干成膜后将 PVDF 薄膜放置在位移台上，控制位移台使激光在 PVDF 表面进行单向线扫描，激光功率为 1200 mW。然后，采用 CLSM 观察 PVDF 与 L-PVDF 薄膜表面。图 2(c)为 PVDF 薄膜的表面形貌图像，PVDF 薄膜通过自身流动性摊开及烘干得到，烘干过程中，DMF 挥发留下 PVDF 成膜，因此表面有一定的起伏感。图 2(d)为 L-PVDF 薄膜的表面形貌。与图 2(c)相比，激光加工过程将原来的表面破坏，激光沿着其扫描路径留下沟槽；同时由于激光的光热效应，使沟槽周围区域形貌也变得粗糙。沟槽和沟槽周围/表面粗糙的结构有利于减少 L-PVDF 表面和水滴的接触面积。

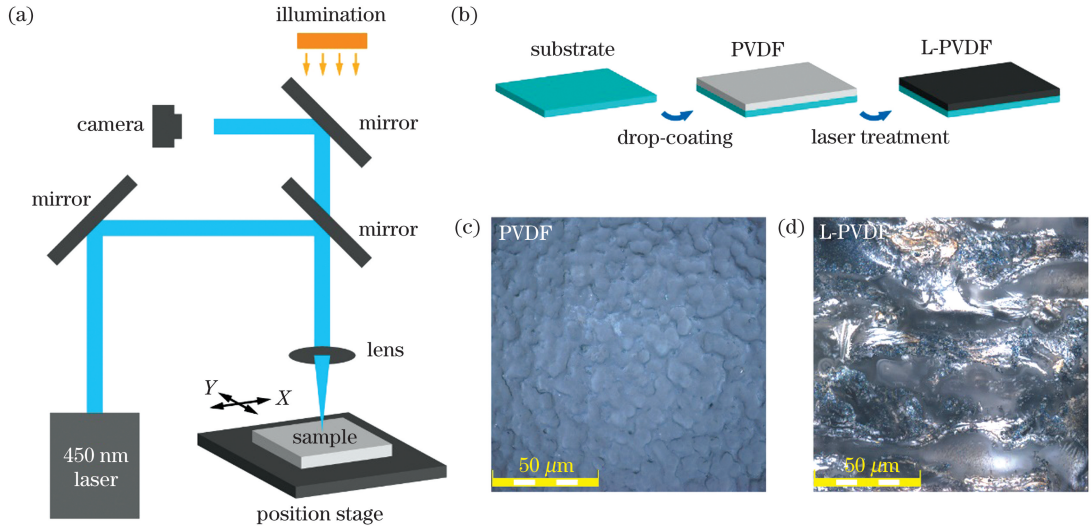

图 2　PVDF 的激光加工处理。(a)激光加工系统；(b)激光处理 PVDF 的示意图；(c)PVDF 薄膜的表面；(d)L-PVDF 薄膜表面

Fig. 2　Laser processing of PVDF. (a) Laser processing system; (b) schematic diagram of laser processing PVDF; (c) surface of PVDF film; (d) surface of L-PVDF film

用 SEM 对 PVDF 和 L-PVDF 薄膜表面结构进行观察分析，结果如图 3 所示。图 3(a)、图 3(b)为 PVDF 薄膜表面的 SEM 图像，可以发现，薄膜表面存在小孔、凹陷等不规则结构，原因是 DMF 溶剂的挥发。图 3(c)～图 3(f)为 L-PVDF 薄膜的 SEM 图像，从图 3(c)可以观察到明显的线性扫描路径，沟槽间距约为 100 μm，沟槽宽度约为 70 μm。图 3(d)为沟槽内部的放大图，可以观察到 L-PVDF 材料沟槽内部也存在粗糙结构。图 3(e)、图 3(f)为 L-PVDF 薄膜表面大量的颗粒状物体，尺寸约为 1 μm，这些颗粒与荷叶表面的乳突尺寸接近(荷叶表面的乳突直径约为 3～5 μm)，且处于同一量级。但 L-PVDF 表面的凸起更紧凑，有利于提高粗糙度。因此，在微纳结构方面，L-PVDF 薄膜具有类似荷叶表面的结构，使 L-PVDF 薄膜具有与荷叶类似的疏水性质。

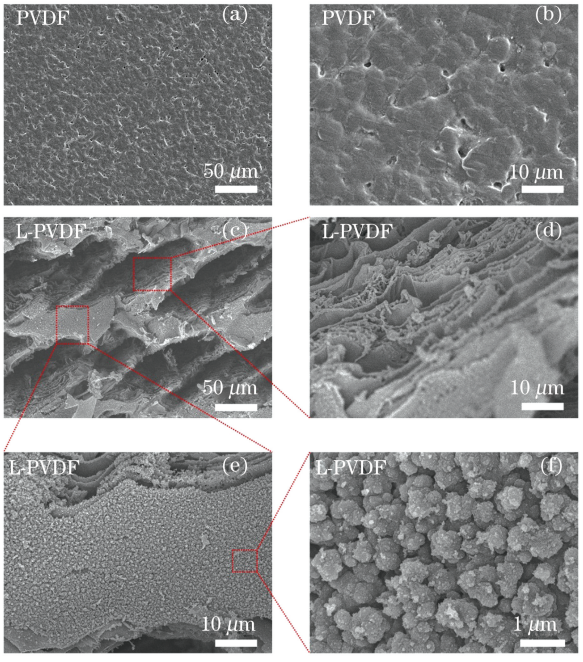

图 3　PVDF 及 L-PVDF 薄膜表面的 SEM 图像。(a)～(b) PVDF 薄膜；(c)～(f) L-PVDF 薄膜

Fig. 3　SEM images of the surface of PVDF and L-PVDF films. (a)-(b) PVDF films; (c)-(f) L-PVDF films

3.3　PVDF 与 L-PVDF 的成分对比

材料表面的浸润性主要由微纳结构和化学组分两部分决定。为了详细分析经激光处理前后 PVDF

的表面组分变化，分别对 PVDF 和 L-PVDF 进行 XPS 测试。PVDF 薄膜表面的碳元素含量（原子数分数）约为 52.27%，氟元素含量约为 47.24%，碳元素与氟元素含量的比值为 1.2，如图 4(a)所示（1 s 为原子中 1 s 轨道电子被激发测得的光电子能量）。而 L-PVDF 薄膜表面的碳元素含量约为 86.84%，氟元素含量约为 7.54%，碳元素与氟元素含量的比值为 11.5，如图 4(b)所示。这表明经过激光处理后，L-PVDF 表面具有更多的碳元素含量，氟含量减少。进一步分析 PVDF 和 L-PVDF 材料薄膜的 C1s 谱图，结果如图 4(c)、图 4(d)所示。可以发现，PVDF 的 C1s 包含两个强度大致相同的主峰，分别为—CF_2—（结合能为 289.1 eV）和—CH_2—（结合能为 284.6 eV），符合 PVDF 的主要化学结构。激光处理后，PVDF 位于 289.1 eV 的峰（主要代表为—CF_2—）明显降低，这表明 C—F 键发生断裂，即 PVDF 材料的分子链结构被激光破坏，碳元素与氟元素含量的比值由 1.2 提高至 11.5[37-40]。

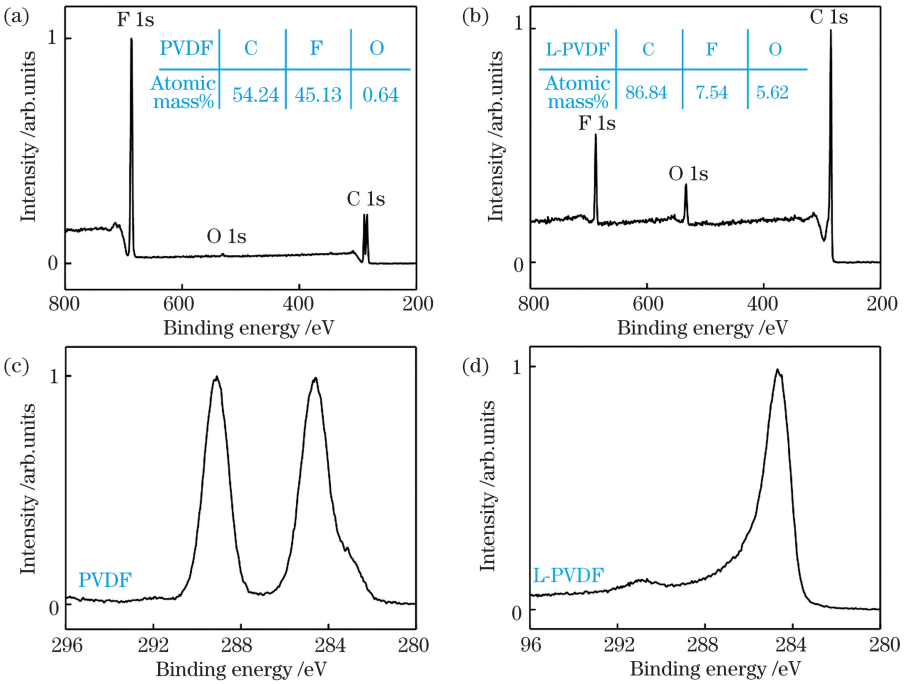

图 4 PVDF 的 XPS 谱图。(a) PVDF 薄膜；(b) L-PVDF 薄膜表面的 XPS 宽谱图；(c) PVDF 薄膜；(d) L-PVDF 薄膜表面的 C1s 谱图

Fig. 4 XPS spectrum of PVDF. (a) PVDF film; (b) XPS broad spectrum of L-PVDF film surface; (c) PVDF film; (d) C1s spectrum of L-PVDF film surface

3.4 PVDF 与 L-PVDF 表面疏水性能的对比

图 5 为接触角测量仪对 PVDF 和 L-PVDF 薄膜表面水滴静态接触角的测量结果，图 5(a)为不同激光功率处理后 L-PVDF 薄膜表面的水滴静态接触角，图 5(b)为用半导体连续激光器处理后 L-PVDF 薄膜表面的水滴静态接触角。用不同激光功率（300～2700 mW，间隔为 300 mW）对 PVDF 薄膜进行处理，结果表明，当激光功率小于 1200 mW 时，激光并未对 PVDF 薄膜产生作用；当激光功率大于 1200 mW 时，激光在 PVDF 薄膜上加工出与图 3(c)一致的结构。对这些样品进行了疏水性能测试，得到的水滴静态接触角约为 150°，可以认为疏水性能基本一致。L-PVDF 的生成需要一定的能量值，且在能量大于 PVDF 发生改性的激光功率阈值后生成的 L-PVDF 薄膜具有相似的结构，导致不同加工功率下形成的 L-PVDF 薄膜具有大致相同的水滴静态接触角。从加工完整性方面考虑，较强的能量有可能破坏膜上引入的类荷叶表面结构。因此，在疏水性能基本一致的情况下，选择功率为 1200 mW 的激光制备的 L-PVDF 薄膜，并进行实验与测试。图 5(b)为稳定性实验的结果，分别对 PVDF 以及 L-PVDF 薄膜进行了 10 次水滴静态接触角的测量。可以发现，L-PVDF 薄膜表面的水滴静态接触角基本没有变化，稳定在 150°附近，这表明激光加工 PVDF 薄膜可以形成具有稳定微纳结构的超疏水表面。

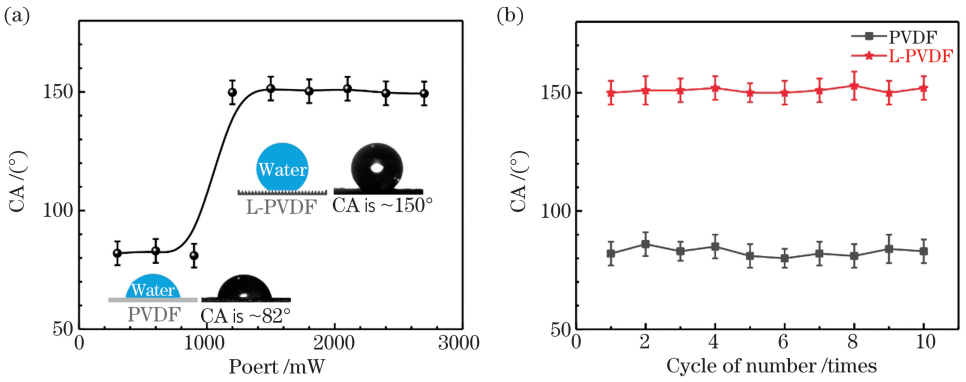

图 5 静态接触角的测试。(a)不同加工功率下的表面静态接触角;(b) 表面静态接触角的稳定性测试

Fig. 5 Test of the static contact angle. (a) Surface static contact angle under different processing power; (b) stability test of the surface static contact angle

4 结 论

受荷叶微观表面的启发,用波长为 450 nm 的半导体连续激光对 PVDF 表面进行加工,结果表明,L-PVDF 表面的水滴静态接触角可达到 150°,具有很好的超疏水性质。同时连续对 L-PVDF 进行静态接触角测试,结果都稳定在 150°附近,具有很好的稳定性。通过 CLSM 和 SEM 对薄膜的微观结构进行表征,结果表明,激光扫描路径形成的沟槽以及激光热效应形成的微小颗粒状结构使 L-PVDF 表面具有与荷叶表面类似的粗糙结构,这种结构减小了水滴与表面的接触面积。结合 XPS 分析得到的结果表明,激光处理前后,材料表面碳元素与氟元素含量的比值由 1.2 提高至 11.5。采用激光加工制备 PVDF 超疏水表面的方法高效便捷,处理过程简便且不涉及化学试剂,为制备 PVDF 超疏水表面提供了新思路。

参 考 文 献

[1] Long J Y, Fan P X, Gong D W, et al. Ultrafast laser fabricated bio-inspired surfaces with special wettability [J]. Chinese Journal of Lasers, 2016, 43(8): 0800001.
龙江游, 范培迅, 龚鼎为, 等. 超快激光制备具有特殊浸润性的仿生表面[J]. 中国激光, 2016, 43(8): 0800001.

[2] Liu M J, Wang S T, Jiang L. Nature-inspired superwettability systems [J]. Nature Reviews Materials, 2017, 2: 17036.

[3] Zhang J Z, Chen F, Yong J L, et al. Research progress on bioinspired superhydrophobic surface induced by femtosecond laser [J]. Laser & Optoelectronics Progress, 2018, 55(11): 110001.
张径舟, 陈烽, 雍佳乐, 等. 飞秒激光诱导仿生超疏水材料表面的研究进展[J]. 激光与光电子学进展, 2018, 55(11): 110001.

[4] Wang S, Liu K, Yao X, et al. Bioinspired surfaces with superwettability: new insight on theory, design, and applications [J]. Chemical Reviews, 2015, 115(16): 8230-8293.

[5] Han D D, Zhang Y L, Jiang H B, et al. Moisture-responsive graphene paper prepared by self-controlled photoreduction[J]. Advanced Materials, 2015, 27(2): 332-338.

[6] Wang L, Chen Q D, Cao X W, et al. Plasmonic nano-printing: large-area nanoscale energy deposition for efficient surface texturing [J]. Light: Science & Applications, 2017, 6(12): e17112.

[7] Yang J, Luo F F, Kao T S, et al. Design and fabrication of broadband ultralow reflectivity black Si surfaces by laser micro/nanoprocessing [J]. Light: Science & Applications, 2014, 3(7): e185.

[8] Sugioka K, Cheng Y. Ultrafast lasers-reliable tools for advanced materials processing [J]. Light: Science & Applications, 2014, 3(4): e149.

[9] You R, Liu Y Q, Hao Y L, et al. Laser fabrication of graphene-based flexible electronics [J]. Advanced Materials, 2020, 32(15): 1901981.

[10] Shi Y, Xu B, Wu D, et al. Research progress on fabrication of functional microfluidic chips using femtosecond laser direct writing technology [J]. Chinese Journal of Lasers, 2019, 46(10): 1000001.
史杨, 许兵, 吴东, 等. 飞秒激光直写技术制备功能化微流控芯片研究进展[J]. 中国激光, 2019, 46(10): 1000001.

[11] Wu D, Xu J, Niu L G, et al. In-channel integration of designable microoptical devices using flat scaffold-supported femtosecond-laser microfabrication for coupling-free optofluidic cell counting [J]. Light: Science & Applications, 2015, 4(1): e228.

[12] Han D D, Zhang Y L, Ma J N, et al. Light-mediated manufacture and manipulation of actuators [J].

Advanced Materials, 2016, 28(38): 8328-8343.

[13] Zhang Y L, Liu Y Q, Han D D, et al. Quantum-confined-superfluidics-enabled moisture actuation based on unilaterally structured graphene oxide papers[J]. Advanced Materials, 2019, 31(32): 1901585.

[14] Fu X Y, Chen Z D, Han D D, et al. Laser fabrication of graphene-based supercapacitors[J]. Photonics Research, 2020(4): 577-588.

[15] Han D D, Chen Z D, Li J C, et al. Airflow enhanced solar evaporation based on Janus graphene membranes with stable interfacial floatability[J]. ACS Applied Materials & Interfaces, 2020, 12(22): 25435-25443.

[16] Han D D, Cai Q, Li J C, et al. Preparation of laser induced graphene based underwater superoleophobic bionic surface[J]. Laser & Optoelectronics Progress, 2020, 57(15): 151408.
韩冬冬, 蔡青, 李纪超, 等. 激光诱导石墨烯水下超疏油仿生表面的制备[J]. 激光与光电子学进展, 2020, 57(15): 151408.

[17] Jiang Y, Jiang Y, Zhang L C, et al. Non-diaphragm fiber gas pressure sensor based on femtosecond laser machining[J]. Laser & Optoelectronics Progress, 2019, 56(10): 100601.
姜源, 江毅, 张柳超, 等. 基于飞秒激光加工的无膜光纤气体压力传感器[J]. 激光与光电子学进展, 2019, 56(10): 100601.

[18] Zou T T, Zhao B, Xin W, et al. High-speed femtosecond laser plasmonic lithography and reduction of graphene oxide for anisotropic photoresponse[J]. Light: Science & Applications, 2020, 9: 69.

[19] Li Z Z, Wang L, Fan H, et al. O-FIB: far-field-induced near-field breakdown for direct nanowriting in an atmospheric environment[J]. Light: Science & Applications, 2020, 9: 41.

[20] Salter P S, Booth M J. Adaptive optics in laser processing[J]. Light, Science & Applications, 2019, 8: 110.

[21] Jiang L, Wang A D, Li B, et al. Electrons dynamics control by shaping femtosecond laser pulses in micro/nanofabrication: modeling, method, measurement and application[J]. Light: Science & Applications, 2018, 7(2): 17134.

[22] Liu K C, Zhang Z Y, Shan C X, et al. A flexible and superhydrophobic upconversion-luminescence membrane as an ultrasensitive fluorescence sensor for single droplet detection[J]. Light: Science & Applications, 2016, 5(8): e16136.

[23] Li J J, Liu Y, Qu S L. Research progress on optical fiber functional devices fabricated by femtosecond laser micro-nano processing[J]. Laser & Optoelectronics Progress, 2020, 57(11): 111402.
李金健, 刘一, 曲士良. 飞秒激光微纳加工光纤功能器件研究进展[J]. 激光与光电子学进展, 2020, 57(11): 111402.

[24] Malinauskas M, Zukauskas A, Hasegawa S, et al. Ultrafast laser processing of materials: from science to industry[J]. Light: Science & Applications, 2016, 5(8): e16133.

[25] Chen Z D, Li J C, Xiao S L, et al. Laser reduced graphene oxide for thin film flexible electronic devices[J]. Laser & Optoelectronics Progress, 2020, 57(11): 111428.
陈招弟, 李纪超, 萧善霖, 等. 激光还原氧化石墨烯制备薄膜柔性电子器件[J]. 激光与光电子学进展, 2020, 57(11): 111428.

[26] Yuan Z Q, Chen H, Tang J X, et al. A novel preparation of polystyrene film with a superhydrophobic surface using a template method[J]. Journal of Physics D Applied Physics, 2007, 40(11): 3485.

[27] Oktay B, Toker R D, Kayaman-Apohan N. Superhydrophobic behavior of polyimide-siloxane mats produced by electrospinning[J]. Polymer Bulletin, 2015, 72(11): 2831-2842.

[28] Gong D W, Long J Y, Jiang D F, et al. Robust and stable transparent superhydrophobic polydimethylsiloxane films by duplicating via a femtosecond laser-ablated template[J]. ACS Applied Materials & Interfaces, 2016, 8(27): 17511-17518.

[29] Wang W, Liu Y Q, Liu Y, et al. Direct laser writing of superhydrophobic PDMS elastomers for controllable manipulation via Marangoni effect[J]. Advanced Functional Materials, 2017, 27(44): 1702946.

[30] Zhang Y L, Ma J N, Liu S, et al. A "Yin"-"Yang" complementarity strategy for design and fabrication of dual-responsive bimorph actuators[J]. Nano Energy, 2020, 68: 104302.

[31] Chen F Z, Lu Y, Liu X, et al. Table salt as a template to prepare reusable porous PVDF-MWCNT foam for separation of immiscible oils/organic solvents and corrosive aqueous solutions[J]. Advanced Functional Materials, 2017, 27(41): 1702926.

[32] Li D K, Gou X L, Wu D H, et al. A robust and stretchable superhydrophobic PDMS/PVDF @ KNFs membrane for oil/water separation and flame retardancy[J]. Nanoscale, 2018, 10(14): 6695-6703.

[33] Liu T, Li X F, Wang D H, et al. Superhydrophobicity and regeneration of PVDF/SiO_2 composite films[J]. Applied Surface Science, 2017, 396: 1443-1449.

[34] Wu J D, Ding Y J, Wang J Q, et al. Facile fabrication of nanofiber- and micro/nanosphere-coordinated PVDF membrane with ultrahigh permeability of viscous water-in-oil emulsions[J]. Journal of Materials

Chemistry A, 2018, 6(16): 7014-7020.
[35] Han D D, Cai Q, Chen Z D, et al. Bioinspired surfaces with switchable wettability [J]. Frontiers in Chemistry, 2020, 8: 692.
[36] Zhang P C, Lin L, Zang D M, et al. Designing bioinspired anti-biofouling surfaces based on a superwettability strategy [J]. Small, 2017, 13(4): 1503334.
[37] Viswanath P, Yoshimura M. Light-induced reversible phase transition in polyvinylidene fluoride-based nanocomposites [J]. SN Applied Sciences, 2019, 1(11): 1-9.
[38] Bartnik A, Fiedorowicz H, Jarocki R, et al. Efficient micromachining of poly(vinylidene fluoride) using a laser-plasma EUV source [J]. Applied Physics A, 2012, 106(3): 551-555.
[39] Sultana T, Georgiev G L, Auner G, et al. XPS analysis of laser transmission micro-joint between poly(vinylidene fluoride) and titanium [J]. Applied Surface Science, 2008, 255(5): 2569-2573.
[40] Chakradhar R P S, Prasad G, Bera P, et al. Stable superhydrophobic coatings using PVDF-MWCNT nanocomposite [J]. Applied Surface Science, 2014, 301: 208-215.

Laser Processing of Polyvinylidene Fluoride with Superhydrophobicity

Li Jichao[1], Chen Zhaodi[1], Han Dongdong[1*], Zhang Yonglai[1], Sun Hongbo[2]

[1] *State Key Laboratory of Integrated Optoelectronics, College of Electronic Science and Engineering, Jilin University, Changchun, Jilin* 130012, *China*;

[2] *State Key Laboratory of Precision Measurement Technology & Instruments, Department of Precision Instrument, Tsinghua University, Beijing* 100084, *China*

Abstract

Objective Various bioinspired surfaces about super-wettability have been widely investigated. For example, water droplets move freely on the lotus leaf surface, in an anisotropic way on rice leaf surfaces, and unidirectionally on pitcher surfaces. With the progress of science and technology, the mechanisms for these bioinspired surfaces have been revealed. Importantly, bioinspired surfaces have abroad applications in biological, industrial, micromechanical, and other fields. For example, superhydrophobic surfaces, requiring high roughness and low surface energy, show self-cleaning and anti-icing characteristics. From the view of materials, organic polymer materials have lower surface energy than other materials, showing great potential in developing superhydrophobic surfaces. As a typical polymer material, polyvinylidene fluoride (PVDF) shows excellent flexibility, chemical corrosion resistance, and piezoelectricity. Superhydrophobic PVDF has recently been prepared by various methods, such as hybrid modification and surface chemistry modification. However, these methods require special chemical reagents or complicated equipment. Herein, we designed and fabricated PVDF-based membranes with superhydrophobicity by laser processing technology. After the laser treatment, the laser treated-PVDF (L-PVDF) surface owns microstructures and low surface energy. Therefore, the L-PVDF surface shows superhydrophobicity. This work provides a new method to prepare the PVDF membrane with excellent superhydrophobicity.

Methods PVDF powders and N, N—dimethylformamide (DMF) solvent are mixed in the ratio of 1 g∶8 ml. After ultrasonic treatment for 1 h, the PVDF powder is uniformly dispersed. The PVDF@DMF solution is drop-coated on substrates to fabricate PVDF membranes. As for the preparation of L-PVDF surfaces, a continuous semiconductor laser wavelength (λ = 450 nm, power P = 1200 mW) is used. After the laser treatment, the L-PVDF surface shows superhydrophobic characteristc. The morphologies of lotus leaf, PVDF, and L-PVDF surfaces are measured by a confocal laser scanning microscope (CLSM) and a scanning electron microscope (SEM). The chemical compositions of the PVDF and L-PVDF are analyzed by X-ray photoelectron spectroscopy (XPS). The surface wettability and wettability stability of the PVDF and L-PVDF are characterized by a static contact angle (CA) measuring system. For the CA measurement, the area of laser treatment is 10 mm × 10 mm, and the processing time is about 3 min.

Results and Discussion The static CA of water drops on a lotus leaf is ~150°, indicating superhydrophobic characteristic. To explore the mechanism of the superhydrophobic characteristic of water droplets on the lotus leaf surface, we characterized the lotus leaf surface morphology by the CLSM and SEM, respectively. There are microscaled papillae with a diameter of 3–5 μm and a height of 5–10 μm (**Fig. 1**). The existence of microscaled

papillae can effectively reduce the contact area between water droplets and lotus leaf surfaces, leading to the superhydrophobic effect. **Fig. 2** shows the laser processing system and the procedure of laser processing PVDF surface. The SEM images show that there are grooves along the laser scanning path. The distance between grooves is ~100 μm, and the width is ~70 μm. Moreover, many particles (diameter is ~ 1 μm) are observed. The size and shape of particles are similar to the papillae on a lotus leaf (**Fig. 3**). Besides, XPS is performed to investigate the change of surface composition of PVDF and L-PVDF surface. The C/F atom ratio has significantly changed from 1.2 (PVDF) to 11.5 (L-PVDF), which indicates that the molecular chain of PVDF is destroyed by high laser power, and defluorination may occur (**Fig. 4**). Compared with the CA of PVDF film (~ 82°), the L-PVDF surface shows hydrophobicity with a CA of ~ 150°(**Fig. 5**).

Conclusions Inspired by the microstructures on the lotus leaf surfaces, a L-PVDF-based superhydrophobic surface has been prepared by a continuous semiconductor laser (λ = 450 nm, P = 1200 mW). CLSM and SEM are used to characterize the microstructure of L-PVDF. Grooves and microscaled papillae are induced fabrication by the laser thermal effect. The microstructures on the surface of L-PVDF is similar to that of the lotus leaf surface. Besides, the rough structure reduces the contact area between water droplets and the L-PVDF surface. XPS reveals that the C/F atom ratio on the surface increased from 1.2 (PVDF) to 11.5 (L-PVDF). Therefore, the CA of L-PVDF is mainly dependent on the change of microstructures and composition. The static CA on the L-PVDF surface is ~150°. This work shows the fabrication of superhydrophobic L-PVDF films by laser processing. The laser processing is simple and does not involve chemical reagents. We deem that this method provides a new strategy to prepare a PVDF-based superhydrophobic surface.

Key words laser technique; polyvinylidene fluoride; superhydrophobicity; biomimetic surface; micro-nano structure

OCIS codes 140.3390; 140.3450; 140.5960